

# Saturated absorption in acetylene and hydrogen cyanide in hollow-core photonic bandgap fibers

Jes Henningsen, Jan Hald, and Jan C. Petersen

Danish Fundamental Metrology, Matematiktorvet B307,  
DK 2800 Kgs. Lyngby, Denmark

[jh@dfm.dtu.dk](mailto:jh@dfm.dtu.dk)

**Abstract:** Saturated absorption is studied in overtone transitions of  $C_2H_2$  and  $H^{13}CN$  molecules confined in the hollow core of a photonic bandgap fiber. The dynamics of filling and venting the fiber is markedly different for the two molecules owing to the presence of a permanent dipole moment in one of them. Saturation is observed for input power down to 10 mW, and well resolved Lamb dips limited by transit time broadening across the 10  $\mu m$  core diameter are observed with a counter-propagating probe beam.

© 2005 Optical Society of America

**OCIS codes:** (060.2400) Fiber optics; (120.3930) Metrological instruments; (230.3990) Microstructure devices; (300.6460) Saturation; (350) Optical standards

---

## References and links

1. R. F. Cregan, B. J. Mangan, J. C. Knight, T. A. Birks, P. St. J. Russell, P. J. Roberts, and D. C. Allan, "Single-Mode Photonic Bandgap Guidance of Light in Air," *Science* **285**, 1537-1539 (1999).
2. P. J. Roberts, F. Couny, H. Sabert, B. J. Mangan, D. P. Williams, L. Farr, M. W. Mason, A. Tomlinson, T. A. Birks, J. C. Knight, and P. St. J. Russell, "Ultimate low loss of hollow-core photonic crystal fibers," *Opt. Express* **13**, 236-244 (2005).
3. T. Ritari, J. Tuominen, H. Ludvigsen, J. C. Petersen, T. Sørensen, T. P. Hansen, and H. R. Simonsen, "Gas sensing using air-guiding photonic bandgap fibers," *Opt. Express* **12**, 4080-4087 (2004).
4. J. Tuominen, T. Ritari, H. Ludvigsen, J. C. Petersen, "Gas filled photonic bandgap fibers as wavelength references," *Opt. Commun.* **255**, 272-277 (2005).
5. F. Benabid, F. Couny, J. C. Knight, T. A. Birks, and P. St. J. Russell, "Compact, stable and efficient all-fiber gas cells using hollow-core photonic crystal fibers," *Nature* **434**, 488-491 (2005).
6. S. Ghosh, J. E. Sharping, D. G. Ouzounov, and A. L. Gaeta, "Resonant Optical Interactions with Molecules Confined in Photonic Band-Gap Fibers," *Phys. Rev. Lett.* **94**, 093902 (2005).
7. F. Benabid, P. S. Light, F. Couny, and P. S. Russell, "Electromagnetically-induced transparency grid in acetylene-filled hollow-core PCF," *Opt. Express* **13**, 5694-5703 (2005).
8. M. Faheem, R. Thapa, and K. L. Corwin, "Spectral hole burning of acetylene gas inside a photonic bandgap optical fiber," Conference of Lasers and Electro Optics CLEO 2005, Long Beach Calif., May 2005.
9. <http://www.crystal-fibre.com>.
10. K. Nakagawa, M. de Labachellerie, Y. Awaji, M. Kourogi, "Accurate optical frequency atlas of the 1.5- $\mu m$  bands of acetylene," *J. Opt. Soc. Am. B* **13**, 2708-2714 (1996).
11. A. Yariv, *Quantum Electronics* (John Wiley & sons, 1988), Chap. 8.
12. K. Saitoh, N. A. Mortensen, and M. Koshiba, "Air-core photonic band-gap fibers: the impact of surface modes," *Opt. Express* **12**, 394-400 (2004).
13. J. A. West, C. M. Smith, N. F. Borrelli, D. C. Allan, and K. W. Koch, "Surface modes in air-core photonic band-gap fibers," *Opt. Express* **12**, 1485-1496 (2004).
14. W. C. Swann and S. L. Gilbert, "Line centers, pressure shift and pressure broadening of 1530-1560 nm hydrogen cyanide wavelength calibration lines," *J. Opt. Soc. Am. B*, **22**, 1749-1756 (2005).
15. Mitsuhiro Kusaba and Jes Henningsen, "The  $\nu_1 + \nu_3$  and the  $\nu_1 + \nu_2 + \nu_4^1 + \nu_5^{-1}$  combination bands of  $^{13}C_2H_2$ . Linestrengths, broadening parameters and pressure shifts," *J. Mol. Spectrosc.* **209** (2001).

## 1. Introduction

Conventional optical fibers consist of a core surrounded by a cladding of slightly lower refractive index, and light is confined in the core by total internal reflection at the interface. While this configuration allows for propagation over long distances with low loss, it is not well suited for studying the interaction with gases. The cladding must be removed, and interaction is only possible with the evanescent field, which falls off exponentially outside the solid core. In a hollow-core photonic band-gap fiber (HC-PBG) [1] light is confined by a periodic pattern of holes surrounding a central void. By interference the periodic structure creates a band-gap for electromagnetic waves, akin to the band-gaps experienced by electron waves in a solid. This prevents the light from escaping from the core, and transmission losses down to 1.2 dB/km at 1565 nm has been reported [2].

Admitting a gas to the core of a HC-PBG fiber enables the study of interaction between light and molecules. Ritari et al. [3, 4] observed the  $\nu_1 + \nu_3$  combination band of acetylene, and Benabid et al. [5] reported on fiber cells with acetylene for wavelength standards and on hydrogen filled cells for Raman scattering. The fiber configuration is particularly advantageous for the study of phenomena where a combination of high intensity and long interaction length is required. Ghosh et al. [6] induced changes in the refractive index of an acetylene gas by applying a strong field at an R-branch transition and observed its effect on the propagation of a probe beam tuned to a coupled P-branch transition, and similar studies of electromagnetically induced transparency were conducted by [7]. Recently Faheem et al. [8] reported observation of saturation of acetylene in a pump-probe configuration. In this paper we report on the observation of saturated absorption in acetylene and in C-13 substituted hydrogen cyanide, both of which are useful as wavelength standards on account of their good overlap with the optical communication C-band.

## 2. Experiment

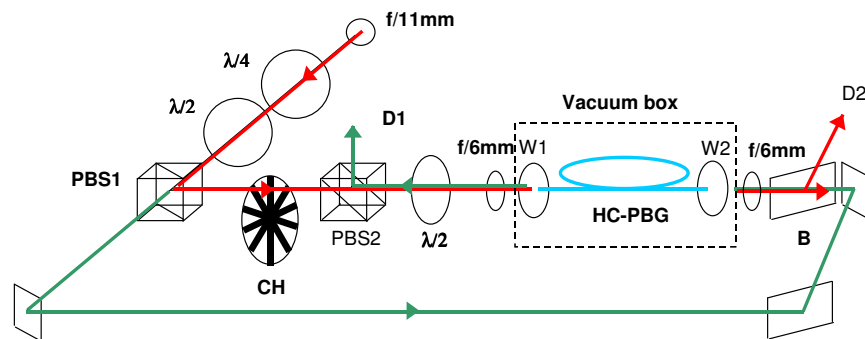


Fig. 1. Experimental configuration for pump-probe configuration with two polarizing beamsplitters PBS1 and PBS2, a chopper CH inserted in the pump beam, a vacuum box with sapphire windows W1 and W2, a thin film beamsplitter BS, and two Ge detectors D1 and D2.

The HC-PBG fiber used in this work, type designation CF-0133 produced by Crystal Fibre

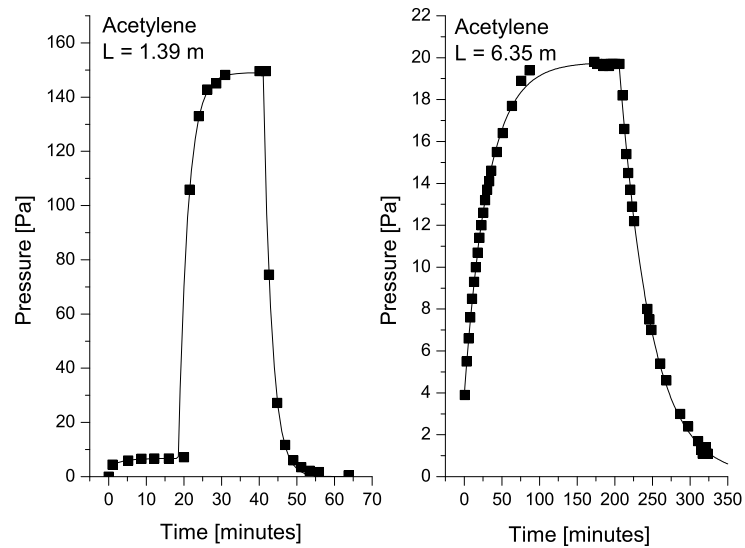


Fig. 2. Average pressure in the fiber during filling and venting with acetylene. Left: Initial filling of 1.39 m fiber to 8.5 Pa, further filling to 149 Pa, and venting. Right: Filling of 6.35 m fiber to 20 Pa and venting.

A/S [9], has a hexagonal cladding with a 7-cell core of  $10\ \mu\text{m}$  diameter. A section of fiber is coiled with a diameter of 6 cm and placed in a vacuum housing, each fiber end accessible through a 1 mm thick AR-coated sapphire window. Radiation from a New Focus extended cavity laser is amplified to 60 mW in an erbium-doped amplifier (EDFA), and focused on the fiber core with a combination of aspheric lenses as shown in Fig. 1. Vacuum is provided by a turbomolecular pump, and the pressure is monitored with a MKS capacitance gauge with 0.1 Pa resolution. The gas was technical acetylene with a nominal purity of 99% or C-13 substituted hydrogen cyanide prepared by the Chemistry Department of the University of Copenhagen.

The radiation emitted from the exit fiber of the EDFA is collimated and reflected towards the fiber by a polarizing beamsplitter PBS1. A  $\lambda/4$  plate ensures linear polarization, and a subsequent  $\lambda/2$  plate provides a convenient means of adjusting the input power to the fiber without affecting the coupling efficiency. The coupling losses of the fiber depend on the polarization, and a second  $\lambda/2$  plate is used for maximising the transmission.

Three different detection schemes are used. In configuration (a), the directly transmitted signal is measured by a  $5\times 5\ \text{mm}^2$  Ge detector positioned close to the window W2 at the exit of the hollow fiber, and the transmitted line profile is measured as a function of the input power. In the second configuration (b), an aspheric lens with 13 mm focal length focuses the exit beam, and a plane mirror positioned at the focal plane retroreflects the beam through the fiber. A mechanical chopper is positioned in front of the retroreflector, and the Ge detector monitors the 670 Hz chopped signal passing from the fiber straight through PBS1 with subsequent demodulation in a lock-in amplifier. In the third configuration (c) shown in Fig. 1, the power transmitted through PBS1 is focused at the fiber exit near W2 with a 6 mm focal length aspheric lens to serve as a counter-propagating probe beam. After leaving the vacuum box through W1 the component polarized perpendicular to the pump beam is reflected by PBS2 and picked up by the Ge de-

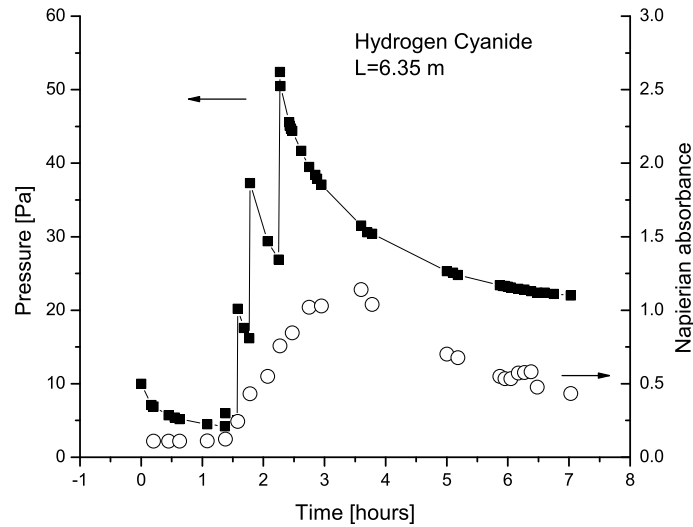


Fig. 3. Filling with hydrogen cyanide. Filled squares indicate the pressure external to the fiber with gas admitted in four steps. Open circles show the absorbance which represents the average pressure in the core of the fiber.

tector D1. The pump is chopped by CH, and the modulation imprinted on the probe beam is detected with the lock-in amplifier. A thin-film beamsplitter BS positioned on the exit side for the pump allows the monitoring of the transmitted signal with the Ge detector D2.

### 3. Filling and venting

Experiments on  $C_2H_2$  were performed on the P9 line of the  $\nu_1 + \nu_3$  band centered at 1530.37095 nm [10]. After evacuating the cell, gas was admitted in the pressure range 5 to 150 Pa, and filling of the fiber was monitored at the transmitted signal by repeatedly scanning the wavelength across the line. According to the Beer-Lambert law, the signal transmitted through a fiber of length  $L$  is given by

$$I(L) = I(0) \exp(-\alpha L) \quad (1)$$

where the absorption coefficient  $\alpha$  is given by

$$\alpha = NSg(\nu - \nu_0) = \frac{p}{kT} Sg(\nu - \nu_0) \quad (2)$$

Here  $N$  is the number of molecules per unit volume,  $S$  is the line strength of the chosen line, and  $g(\nu - \nu_0)$  is the area normalised line shape function. The second relation expresses  $N$  in terms of the pressure  $p$ , the temperature  $T$ , and Boltzmann's constant  $k$ , and we find that in the Doppler limit where the line profile is a Gaussian and independent of pressure, the absorbance  $\alpha L$  as derived from Eq. 1 becomes proportional to the average pressure in the fiber. Note that here and in the following we consistently use the Napierian absorbance.

Figure 2 shows the temporal development of the average fiber pressure during filling and venting of two fibers with  $C_2H_2$ . The pressure development during three steps consisting of initial filling to 8.5 Pa, subsequent refilling to 149 Pa, and eventual venting, are well fitted to

exponentials with time constants of 3.7, 2.6, and 2.3 min, and we thus find that the time constant is essentially independent of pressure and similar for filling and venting. For the 6.35 m fiber we find time constants of 31 min and 41 min for filling and venting respectively, indicating that the time constant increases faster than the fiber length.

The average pressure is determined by measuring the absorbance and converting to pressure with Equation 2. During filling and venting, the pressure is a function of distance along the fiber, with a minimum value at the mid-point, and the average value should thus be interpreted as the constant pressure that leads to the same absorbance as the actual pressure distribution.

After the absorbance has reached a constant value, the pressure in the fiber core must be uniform and equal to the pressure in the vacuum box external to the fiber. This follows since the fiber is symmetrically filled from both ends, and any pressure gradient would imply a transport of molecules into the core and hence be inconsistent with a constant absorbance. Following this line of reasoning it is not necessary to assume the line strength  $S$  to be known. However, in Section 4 we show that the known line strength together with the measured external pressure reproduces the measured absorbance in the unsaturated limit. This constitutes an independent verification that the steady state intra-fiber pressure is indeed equal to the external pressure.

The matrix of holes surrounding the core will necessarily fill at a much slower rate than the core itself. However, this process will not affect the propagation characteristics of the fiber, and since the total volume of the matrix is only a minute fraction of the 900 cm<sup>3</sup> volume of the vacuum box, the effect on the external pressure is not measurable.

In Fig. 3 we show results for H<sup>13</sup>CN in the 6.35 m fiber, using the R7 line of the 2ν<sub>2</sub> overtone band at 1537.300409 nm. Filled squares denote the pressure external to the fiber, reflecting repeated admittance of additional gas. Open circles denote the measured absorbance, which is proportional to the average pressure inside the fiber core. In this case we cannot evaluate the pressure since the line strength has not been measured. We note that the dynamics is strikingly different from what was found for C<sub>2</sub>H<sub>2</sub>, and we attribute this to the fact that H<sup>13</sup>CN has a permanent dipole moment which makes it tend to stick to surfaces. After admittance of gas, the initial spike is followed by a reduction as molecules leave the gas phase and adhere to the surfaces. However, from the measured absorbance we can see that the pressure inside the fiber is not able to respond to these fast variations. From 3.5 hours the absorbance decreases smoothly, following the decreasing pressure in the vacuum box. Between 6 hours and 6.5 hours we reduced the input power by a factor of 5.5 in four steps, and observed an associated increase in absorbance. At 6.5 hours the power was returned to the maximum value, and the absorbance immediately dropped to a value representing an extrapolation of the initial decay. This power dependence of the absorbance constitutes a clear evidence for saturation.

#### 4. Transmission measurements

Using configuration (a), the peak absorbance at a pressure of 10 Pa for the P9 line of C<sub>2</sub>H<sub>2</sub> was determined as a function of the off-line exit power with results as shown in the upper part of Fig. 4. The line strength  $S=1.024 \times 10^{-20}$  cm/mol as determined independently in a conventional absorption cell leads to an unsaturated peak absorbance of  $\alpha_0 L = 0.963$  in good agreement with the low-power limit in Fig. 4.

For an inhomogeneously broadened line the intensity  $I$  along the fiber is given by

$$\frac{dI}{dz} = -\alpha I = \frac{\alpha_0 I}{\sqrt{1 + \frac{I}{I_s}}} \quad (3)$$

where  $I_s$  is the saturation intensity [11], and solving this equation we find that the input intensity  $I_0$  and the output intensity  $I_L$  are related by the expression

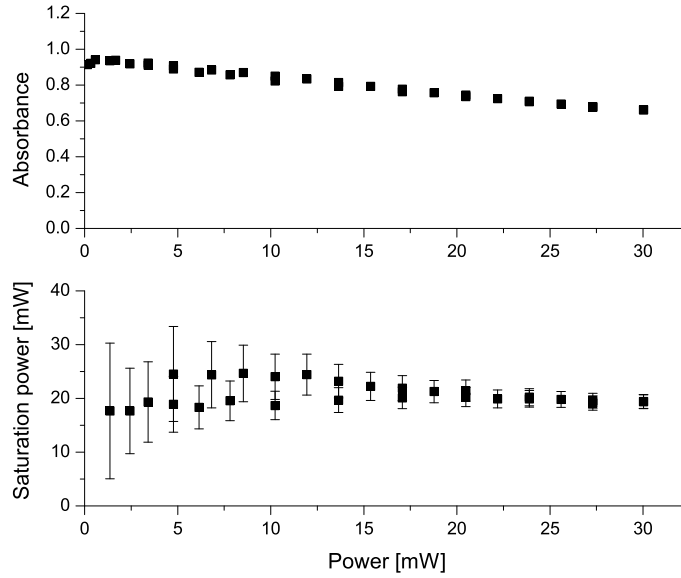


Fig. 4. Peak absorbance for the 6.35 m fiber at 10 Pa (upper) and corresponding saturation power (lower) as a function of the exit power away from the absorption line.

$$\alpha_0 L = 2(\sqrt{1 + I_0/I_s} - \sqrt{1 + I_L/I_s}) + \ln \frac{(\sqrt{1 + I_L/I_s} + 1)(\sqrt{1 + I_0/I_s} - 1)}{(\sqrt{1 + I_L/I_s} - 1)(\sqrt{1 + I_0/I_s} + 1)} \quad (4)$$

Assuming that power and intensity in the fiber are proportional, each combination of input and exit power can then be used for determining a saturation power  $P_s$  with results as given in the lower part of Fig. 4.

The intrinsic loss coefficient of the fiber is 0.2 dB/m, and the average power in the fiber is therefore about 16% higher than the power at the exit, corresponding to a saturation power of 23 mW. In fact it might be slightly lower since the presence of surface modes means that not all of the power transmitted by the fiber contributes effectively to saturation of the molecules.

## 5. Lamb dip measurements

Saturation was further studied by measuring the absorption of a counter-propagating probe beam in configuration (b). Ideally, the retroreflected beam would have the same polarization as the incident beam, and hence be reflected back towards the EDFA by PBS1. However, the fiber shows birefringence so that after two passes the retroreflected beam will be elliptically polarized and therefore partly transmitted, and the left part of Fig. 5 shows the probe signal for  $C_2H_2$  with a clear Lamb dip near the line center. The background oscillations are believed to be caused by surface modes [12, 13], and although they do not prevent the observation of the Lamb dip, they will corrupt a quantitative analysis of the line shape. The oscillations appear because the field carried by the surface modes diverges strongly after exiting the fiber and therefore cannot be retroreflected. Thus, the detected signal becomes sensitive to frequency dependent variations in the relative amount of core mode and surface modes. This is not a problem for

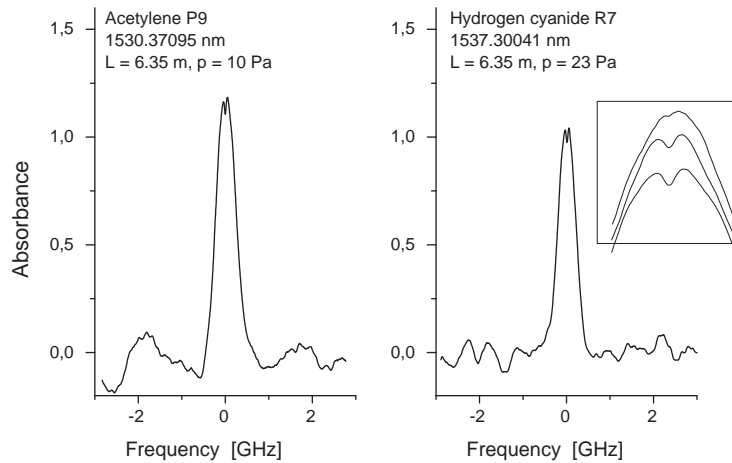


Fig. 5. Lamb dips in acetylene and hydrogen cyanide at an average power in the fiber of 30 mW. The insert shows from above the line center region at an average power of 6 mW, 20 mW, and 30 mW. The background structure is attributed to surface modes.

transmission measurements in configuration (a) where a large-area detector positioned close to the fiber exit will pick up the total transmitted power.

The right part of Fig. 5 shows similar results for  $\text{H}^{13}\text{CN}$  where a somewhat higher pressure is required to obtain a comparable absorbance. The line center positions as well as collisional broadening parameters and pressure shifts have recently been measured by Swann and Gilbert [14]. For the R7 line they report a HWHM collision broadening parameter of 0.32 MHz/Pa corresponding to 7.5 MHz at our pressure of 23.3 Pa, and we are thus safely below the 232 MHz Doppler width.

The result of measurements on acetylene in the configuration (c) are shown in Fig. 6. The upper part shows the transmitted Doppler broadened profile with a peak Napierian absorbance of 0.7 corresponding to an attenuation of the beam by 50%. Although only a 2.5 GHz interval is shown, the Gaussian fit extends over a frequency range of 14 GHz in order to achieve an averaging of the background structure. The lower part shows the saturation signal with a superimposed fit to a Lorentzian of HWHM line width 22.4 MHz, together with the corresponding residual. The width exceeds by far the collision broadening of 0.45 MHz determined from the coefficient 0.045 MHz/Pa given in [15]. It agrees with the width found by Faheem et al. [8] for a similar fiber, and it is very close to the value 21.7 MHz derived from the expression

$$\Delta\nu = 0.444 \frac{u}{L} \quad (5)$$

given in [16] for the HWHM width for transit time broadening, using  $u = \sqrt{8kT/\pi M} = 489.5$  m/s for the mean molecular velocity at 296K, and taking  $L$  as the 10  $\mu\text{m}$  core diameter.

The S/N ratio is limited by background oscillations whose origin have not yet been established. Note that the residual of the Lorentz fit diminishes as the line center is approached because the transmitted power and hence also the background oscillations are reduced due to the absorption. Defining a S/N for a 200 MHz interval centered at the line, we find a value of 26 if the noise is taken as the rms value of the background oscillations.

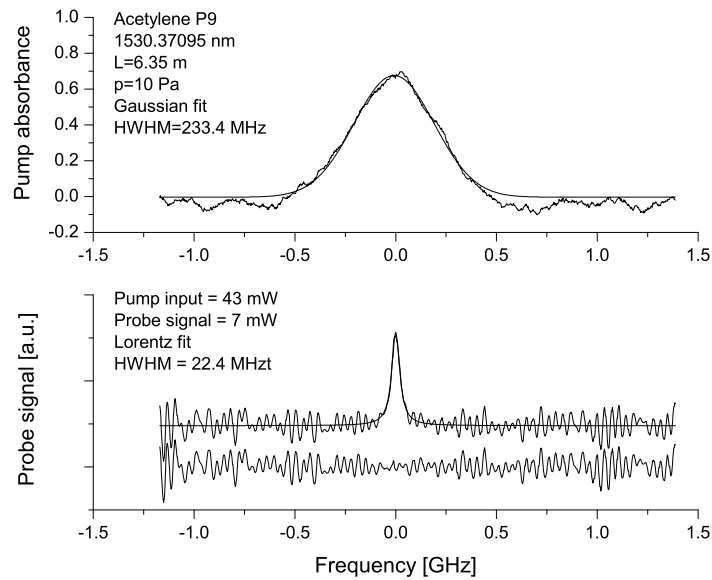


Fig. 6. Pump absorption (upper graph), and Lamb dip (lower graph) in pump-probe configuration. The bottom trace shows the residual of a Lorentz fit.

## 6. Conclusion

We have used hollow-core photonic bandgap fibers for observing saturated absorption on overtone transitions around 1530 nm in  $C_2H_2$  and in  $H^{13}CN$ . The saturation power is about 23 mW, and Lamb dips can be observed down to a power of less than 10 mW in the fiber. The dynamics of filling and venting the fiber is different for the two molecules as a consequence of different adhesion properties. The half width of the Lamb dips is determined by transit time broadening in the fiber core.

Both molecules are popular as wavelength standards in optical communication, and the observation of Lamb dips suggests that a significant improvement over Doppler limited standards is possible. The presence of surface modes represents a problem for a quantitative analysis, since they affect the spatial distribution of intensity over the core cross section, and hence the saturation conditions. In addition, the background oscillations will have an impact on the accuracy with which the Lamb-dip minimum identifies the center of the absorption line, and to realize the full potential of the fibers in connection with wavelength standards, they should be eliminated.

## Acknowledgments

We acknowledge Crystal Fibre A/S for providing the fiber and for sharing their expertise, and the Danish Research Council for Technology and Production Sciences for financial support under project 26-04-0177 Advanced optical fibre technology: novel concepts and applications.